1-1-2024

Phytoplankton thermal trait parameterization alters community structure and biogeochemical processes in a modeled ocean

Stephanie I. Anderson
Massachusetts Institute of Technology

Clara Fronda
Laboratoire de Physique de l'Ecole Normale Supérieure

Andrew D. Barton
Scripps Institution of Oceanography

Sophie Clayton
Old Dominion University

Tatiana A. Rynearson
University of Rhode Island

See next page for additional authors

Citation/Publisher Attribution

Anderson, Stephanie I., Clara Fronda, Andrew D. Barton, Sophie Clayton, Tatiana A. Rynearson, and Stephanie Dutkiewicz. "Phytoplankton thermal trait parameterization alters community structure and biogeochemical processes in a modeled ocean." *Global Change Biology* 30, 1 (2024). doi: 10.1111/gcb.17093.

Phytoplankton thermal trait parameterization alters community structure and biogeochemical processes in a modeled ocean

Keywords

export processes; global change; marine biogeochemistry; marine ecology; model parameterization; phytoplankton; thermal traits

Authors

Stephanie I. Anderson, Clara Fronda, Andrew D. Barton, Sophie Clayton, Tatiana A. Rynearson, and Stephanie Dutkiewicz

Received: 12 June 2023 | Revised: 19 October 2023 | Accepted: 20 November 2023

DOI: 10.1111/gcb.17093

Global Change Biology WILEY

RESEARCH ARTICLE

Phytoplankton thermal trait parameterization alters community structure and biogeochemical processes in a modeled ocean

Stephanie I. Anderson[1] | Clara Fronda[2] | Andrew D. Barton[3] | Sophie Clayton[4] | Tatiana A. Rynearson[5] | Stephanie Dutkiewicz[1]

[1]Department of Earth, Atmospheric and Planetary Sciences, Massachusetts Institute of Technology, Cambridge, Massachusetts, USA

[2]Laboratoire de Physique, Ecole Normale Supérieure, Paris, France

[3]Scripps Institution of Oceanography and Department of Ecology, Behavior and Evolution, San Diego, California, USA

[4]Department of Ocean and Earth Sciences, Old Dominion University, Norfolk, Virginia, USA

[5]Graduate School of Oceanography, University of Rhode Island, Narragansett, Rhode Island, USA

Correspondence
Stephanie I. Anderson, Narragansett, RI, USA.
Email: siander@mit.edu

Stephanie Dutkiewicz, Department of Earth, Atmospheric and Planetary Sciences, Massachusetts Institute of Technology, Cambridge, MA, USA.
Email: stephdut@mit.edu

Present address
Sophie Clayton, Ocean BioGeosciences, National Oceanography Centre, Southampton, UK

Funding information
National Science Foundation, Grant/Award Number: 1638834; Simons Foundation, Grant/Award Number: 549931FY22 and 874777

Abstract

Phytoplankton exhibit diverse physiological responses to temperature which influence their fitness in the environment and consequently alter their community structure. Here, we explored the sensitivity of phytoplankton community structure to thermal response parameterization in a modelled marine phytoplankton community. Using published empirical data, we evaluated the maximum thermal growth rates (μ_{max}) and temperature coefficients (Q_{10}; the rate at which growth scales with temperature) of six key Phytoplankton Functional Types (PFTs): coccolithophores, cyanobacteria, diatoms, diazotrophs, dinoflagellates, and green algae. Following three well-documented methods, PFTs were either assumed to have (1) the same μ_{max} and the same Q_{10} (as in to Eppley, 1972), (2) a unique μ_{max} but the same Q_{10} (similar to Kremer et al., 2017), or (3) a unique μ_{max} and a unique Q_{10} (following Anderson et al., 2021). These trait values were then implemented within the Massachusetts Institute of Technology biogeochemistry and ecosystem model (called Darwin) for each PFT under a control and climate change scenario. Our results suggest that applying a μ_{max} and Q_{10} universally across PFTs (as in Eppley, 1972) leads to unrealistic phytoplankton communities, which lack diatoms globally. Additionally, we find that accounting for differences in the Q_{10} between PFTs can significantly impact each PFT's competitive ability, especially at high latitudes, leading to altered modeled phytoplankton community structures in our control and climate change simulations. This then impacts estimates of biogeochemical processes, with, for example, estimates of export production varying by ~10% in the Southern Ocean depending on the parameterization. Our results indicate that the diversity of thermal response traits in phytoplankton not only shape community composition in the historical and future, warmer ocean, but that these traits have significant feedbacks on global biogeochemical cycles.

KEYWORDS
export processes, global change, marine biogeochemistry, marine ecology, model parameterization, phytoplankton, thermal traits

1 | INTRODUCTION

Phytoplankton are principal contributors to the global carbon cycle (Falkowski et al., 1998) and form the base of most marine food webs (Sherr & Sherr, 1991). They comprise several phylogenetically diverse Phytoplankton Functional Types (PFTs), defined as groups of phytoplankton that share unique physiological and morphological traits (Reynolds et al., 2002), such as silica utilization by diatoms (Litchman & Klausmeier, 2008). These traits contribute to PFT fitness, leading to distinct phytoplankton assemblages across the world's oceans. Which PFTs are present largely determines marine ecosystem structure and function (Le Quéré et al., 2005), as well as the flux of elements to the ocean interior from the surface (Falkowski et al., 2003; Uitz et al., 2010). However, most Earth system models (which include the coupling between the atmosphere, the ocean, and the land) such as those used in the Intergovernmental Panel on Climate Change Coupled Model Intercomparison Projects still include only a few (typically two to three) PFTs (Laufkotter et al., 2015). Yet, there is an increasing recognition and desire to capture the varied roles and contributions of PFTs to biogeochemical cycling, and in ocean-only biogeochemical models, more PFTs are being resolved than ever before (e.g., MARBL-SPECTRA, with nine phytoplankton from three PFTs, Negrete-García et al., 2022; and Darwin with up to 350 phytoplankton from six PFTs, Dutkiewicz et al., 2020; Follows et al., 2007).

Recent analyses of empirically derived phytoplankton growth rates suggest PFTs may also be uniquely characterized by their temperature response traits (Anderson et al., 2021; Kremer et al., 2017), which alter their fitness in different thermal environments. Through over a billion years of evolution (Keeling, 2010), PFTs have differentiated their maximum growth rates and their thermal niches, or the temperatures at which they are viable (Thomas et al., 2016). These differences are partially driven by environmental variability, with thermal traits becoming more divergent between PFTs as temperature variation increases (i.e., poleward; Thomas et al., 2016). These thermal trait differences influence PFT biogeography in the contemporary ocean and could lead to altered community structure with anthropogenic climate change (Anderson et al., 2021), possibly impacting global primary production (Dutkiewicz et al., 2013) and nutrient cycling (Toseland et al., 2013). However, resolving many PFTs, each with distinctive thermal traits, can be computationally difficult. Instead, most models apply a single thermal trait parameterization universally across all modeled phytoplankton (Laufkotter et al., 2015), which may limit their ability to capture finer ecosystem dynamics. New analyses of thermal traits among PFTs (e.g., Anderson et al., 2021) provide an opportunity to evaluate how measured thermal trait variability impacts phytoplankton community structure and estimates of export processes in a modeled ocean.

Here, we evaluated the importance of accounting for these thermal traits in a dynamic ecosystem model where phytoplankton species compete for resources. We focused on two key parameters shown to vary between PFTs: the maximum growth rate (μ_{max}) and the temperature coefficient (Q_{10}), or the rate at which the μ_{max} scales with each 10°C of temperature change (slope). Diverging from previous studies which have used disparate datasets to estimate thermal parameters (e.g., Buitenhuis et al., 2013), here we utilized a single comprehensive phytoplankton growth dataset (Anderson et al., 2021) and three well-established procedures to evaluate phytoplankton thermal responses, allowing for consistency and comparison between methods. PFTs in empirical analyses were either: (1) evaluated as a single entity resulting in a constant μ_{max} and Q_{10} across all phytoplankton (similar to what was done in Eppley, 1972), (2) assessed with PFTs weighted as a factor leading to varied μ_{max} but a constant Q_{10} for all phytoplankton (similar to Kremer et al., 2017), or (3) analyzed independently resulting in a unique μ_{max} and Q_{10} for each PFT (following Anderson et al., 2021). We then explored how each of these approaches altered estimates of model phytoplankton community structure, as well as several key biogeochemical processes, both in a pre-industrial (1860–1880) and a future ocean (2080–2100).

From our analyses, we found that the parameterization of the μ_{max} and Q_{10} did not have a strong effect on low latitude biogeochemical cycling, but did impact the modeled phytoplankton community structures underlying these processes. Our simulations suggested that a high μ_{max} is necessary for the diatoms, while the Q_{10} is most important at high latitudes, where phytoplankton encounter their thermal minima and where changes in competitive abilities are most pronounced. Thus, the way in which the μ_{max} and the Q_{10} are parameterized can impact modeled phytoplankton community structures, especially at high latitudes, and in turn, estimates of biogeochemical processes. Though we cannot directly validate the distribution of all PFTs produced by these methods, as we do not have the observational data needed for such analyses, we provide illustrative examples of each parameterization in our global simulations and outline when thermal traits may be more important for structuring ecosystem models. This will allow greater certainty in thermal parameterizations, leading to more realistic global ecosystem models.

2 | MATERIALS AND METHODS

2.1 | Global plankton community, biogeochemical, and circulation models

We used a modified version of the plankton community model outlined in Follett et al. (2022) to evaluate the impact of thermal traits on estimates of global phytoplankton community composition and biogeochemical processes. The model includes 31 phytoplankton phenotypes from six PFTs (Dutkiewicz et al., 2021): 2 cyanobacteria, 2 green algae (picoeukaryotes), 5 coccolithophores, 5 diazotrophs, 9 diatoms, and 8 mixotrophic dinoflagellates (Figure S1). Collectively, the phytoplankton phenotypes cover 14 size classes ranging from 0.6 to 104 μm equivalent spherical diameter (ESD) and are distributed evenly on a logarithmic scale following established practices (e.g., Ward et al., 2012), so that the large range of sizes that phytoplankton cover can be captured. The model also includes heterotrophic

bacteria (Follett et al., 2022), and zooplankton that graze on prey following a Holling II function (Holling, 1965). In addition to the biological components, the model simulates biogeochemical cycling of C, N, P, Si and Fe through inorganic and organic forms, as phytoplankton take up nutrients and heterotrophic bacteria recycle them through remineralization (Dutkiewicz, Hickman, et al., 2015; Follett et al., 2022). Each of these biological and biogeochemical components are advected and mixed by the three-dimensional Massachusetts Institute of Technology general circulation model (MITgcm; Marshall et al., 1997). This configuration has a coarse resolution of 2° by 2.5° horizontally and 22 vertical levels that range from 10 m at the surface to 500 m at depth (Monier et al., 2018).

2.2 | Model thermal growth parameters

Phytoplankton growth rates within the plankton community model are calculated as a function of nutrient (*N*) acquisition traits unique to each PFT (Dutkiewicz et al., 2020), irradiance (*I*), and temperature dependency (*T*) according to the following equation:

$$\mu = \mu_{max} \cdot \gamma_T \cdot \gamma_N \cdot \gamma_I. \quad (1)$$

The maximum growth rates (μ_{max}) are scaled allometrically (Table S1: a_PCmax, allometrically scaled carbon-specific growth maximum), as a power law function of cell biovolume based on modeled ESD (Figure S1), where phytoplankton growth rate decreases with size for phenotypes larger than 3 µm, and increases with size for phenotypes smaller than 3 µm (Dutkiewicz et al., 2020; Follett et al., 2022). This unimodal distribution has been observed in laboratory studies (e.g., Marañón et al., 2013) and is likely caused by non-scalable components of the cell (see discussions in Raven, 1994; Ward et al., 2017). For this iteration of the model, we modified the temperature-growth relationship (γ_T), by altering each PFT's temperature coefficient (Q_{10}), as well as their maximum growth rates (μ_{max}), following the three methodologies discussed below. By altering these parameters, we were able to evaluate the impact of thermal traits on estimates of global phytoplankton community composition and biogeochemical processes. Because the Q_{10} is boundless, we also compared the μ_{max} at a single temperature, here 20°C (μ_{max20}; Table 1), though this selection is purely illustrative.

2.3 | Model parameterization using empirical data

To parameterize the temperature coefficients of each PFT, we compiled empirical growth measurements from coccolithophores ($n = 202$), cyanobacteria ($n = 502$), diatoms ($n = 1794$), diazotrophs ($n = 144$), dinoflagellates ($n = 748$), and green algae ($n = 175$). We began with the thermal growth rate compilation by Anderson et al. (2021), and added data from Kremer et al. (2017) to represent green algae and diazotrophs. We then evaluated the Q_{10} by fitting 99th quantile regressions to log-transformed growth rates to capture the growth maxima, as is commonly implemented in phytoplankton biology (Bissinger et al., 2008; Kremer et al., 2017). In curve fitting, we followed three separate methods to assess the importance of varied Q_{10} and μ_{max} on phytoplankton community composition and productivity. First, in the "Eppley" method (Eppley, 1972), we evaluated the thermal dependencies of all phytoplankton as a single entity, fitting a 99th quantile regression (Bissinger et al., 2008) to all log-transformed growth rates, which resulted in one Q_{10} and one μ_{max} across all PFTs (Table 1; Figure 1a). Next, in the "Kremer" method (Kremer et al., 2017), we treated each PFT as a factor in model fitting. This resulted in one Q_{10} across all phytoplankton, but

TABLE 1 For each method and Phytoplankton Functional Type (PFT), the number of strains examined (*n*) and total number of discrete growth measurements used in curve fitting (*N*) are shown. The *y*-intercept for each exponential temperature dependency is determined by *a*, and *b* characterizes the rate at which μ_{max} scales with temperature. The *y*-intercept (converted to growth per day), temperature coefficient (Q_{10}), and growth maximum at 20°C (μ_{max20}) are also shown. Note that the Kremer method used a single *b* and Q_{10} value across all PFTs.

Method	PFT	*n*	*N*	*a*	*b*	Q_{10}	*y*-intercept	μ_{max20}
Eppley	All PFTs	265	3565	−0.1614	0.0382	1.46	0.851	1.8269
Kremer	Coccolithophores	30	202	−0.6443	0.0575	1.7772	0.5250	1.6581
	Cyanobacteria	32	502	−1.2341			0.2911	0.9193
	Diatoms	135	1794	−0.3560			0.7005	2.2122
	Diazotrophs	7	144	−1.9337			0.1446	0.4567
	Dinoflagellates	46	748	−1.3490			0.2595	0.8195
	Green algae	15	175	−0.5119			0.5994	1.8929
Anderson	Coccolithophores	30	202	−0.3005	0.0353	1.4191	0.7408	1.4920
	Cyanobacteria	32	502	−1.6614	0.0758	2.1383	0.1899	0.8685
	Diatoms	135	1794	−0.2263	0.0438	1.5527	0.7977	1.9232
	Diazotrophs	7	144	−1.9337	0.0575	1.7772	0.1446	0.4567
	Dinoflagellates	46	748	−1.2356	0.0512	1.6653	0.2905	0.8057
	Green algae	15	175	−0.6671	0.0635	1.8867	0.5132	1.8274

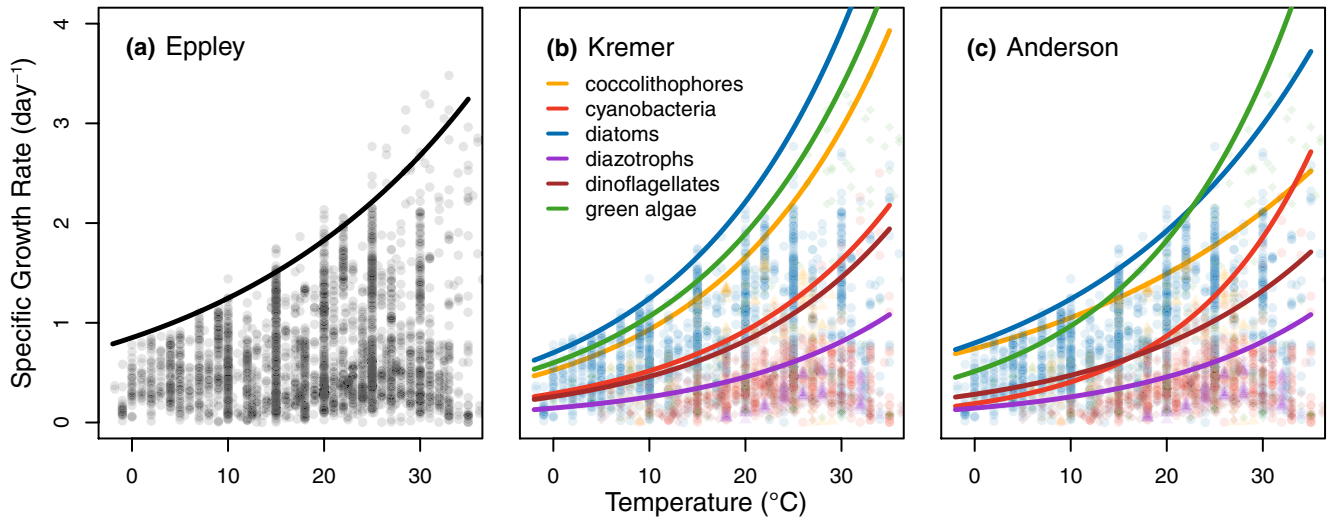

FIGURE 1 Exponential curves characterizing the thermal dependencies of phytoplankton growth according to three documented methods: (a) Eppley (1972), (b) Kremer et al. (2017), and (c) Anderson et al. (2021). Points are empirically derived discrete growth measurements that are the same in each panel but colored based on whether Phytoplankton Functional Types were analyzed together (black, Eppley) or separately (colored, Kremer & Anderson).

unique μ_{max}'s for each PFT (Figure 1b; Figure S2). We adjusted the original method outlined in Kremer et al. (2017), which weighted thermal growth rates by phytoplankton strain to account for differences in the number of growth measurements between strains, and instead weighted by PFT, so no single PFT had a greater influence on the resulting Q_{10}. This better addressed our specific experimental goal of evaluating PFTs and accounted for diatoms being overrepresented in the dataset. Lastly, in the "Anderson" method (Anderson et al., 2021), we assessed thermal growth rates separately for each PFT, which lead to unique estimates of the Q_{10} and μ_{max} for each PFT (Figure 1c; Figure S3; Table 1). For diazotrophs, the data were deemed insufficient for model fitting (Figure S3d; Anderson et al., 2021), so Q_{10} and μ_{max} values were repeated from the Kremer method.

2.4 | Model simulations

Our study was designed to consider the impact of different assumptions about temperature-growth parameterizations on phytoplankton community structure and productivity in the modeled historical and future ocean. The simulations were performed in "offline" mode, in that the physical fields (circulation, mixing, salinity and temperature) were taken from a pre-existing set of Earth system model simulations using a simpler biogeochemical module (Monier et al., 2013) and the Darwin ecosystem component was forced with these. In this offline mode there is no feedback between alteration in the biology, as simulated in this study with Darwin, and the physical fields. These offline fields have been used in several previous studies (Cael et al., 2021; Dutkiewicz et al., 2019; Henson et al., 2021).

Here, we present a series of sensitivity experiments (see Table S2; Anderson, 2023) examining each of the three thermal parameterizations (Eppley, Kremer, and Anderson), under three different ocean environments: a control (based on Greenhouse concentrations in 1860), an ocean warming scenario where temperature (but not the rest of the physics) is as projected for 2080 to 2100 (following the procedure used in Dutkiewicz, Morris, et al., 2015) and a climate change scenario from 2080 to 2100 in which all physical parameters are impacted, including temperature, salinity, and circulation (meridional, zonal, and vertical velocity) under a high emissions scenario. While we focused on the results from the control and climate change simulations, we included the ocean warming only simulation to better distinguish the effects of temperature on phytoplankton community composition from that of other physical parameters which may be altered with climate change, addressing our specific interests in thermal trait parameterization. Each simulation was started from the same initial conditions and run for 20 years; we provide results based on the mean of the last 10 years. Given the number of simulations and the exploratory nature of this study we did not run full 1860 to 2100 simulations. Thus, in the climate change scenarios we will not capture some of the transient features. Instead, we are capitalizing on the large differences in the physical conditions of the control (1860) and the end of century (2080–2100). These differences include large shifts in temperature (up to 5°C difference in sea surface temperature in some locations) and changes in stratification and circulation that lead to significant differences in the supply of nutrients to the euphotic zone.

2.5 | Phytoplankton diversity

We assessed the diversity of the modeled phytoplankton community in the euphotic zone (here presumed to be the uppermost 240 m), averaged over 10 years. We calculated the richness as the

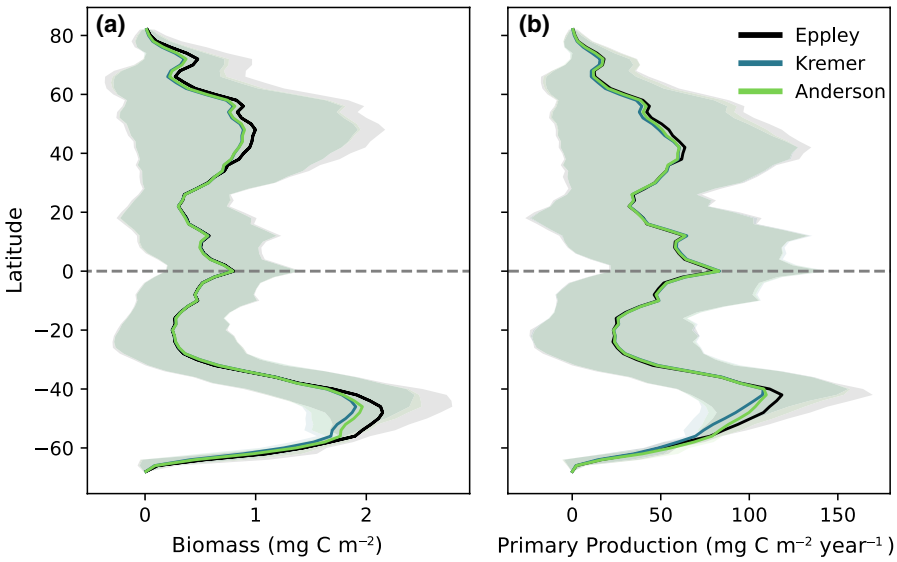

FIGURE 2 Depth-integrated biomass g C m^{-2}; (a) and primary production g C m^{-2} $year^{-1}$; (b) over the upper 240 m from each control simulation averaged over the final 10 years (1870–1880). Lines denote zonal means and shading corresponds to variation across each latitude (±1 SD). Horizontal dashed line indicates the equator.

number of phenotypes comprising greater that 0.001% of the total averaged phytoplankton biomass within a grid cell, as done previously (Barton et al., 2010; Clayton et al., 2013). Evenness (*E*), which describes the distribution of phenotypes within the phytoplankton community, was then discerned using Pielou's evenness metric according to the following equation:

$$E = \frac{-\sum_{i=1}^{R} p_i \ln p_i}{\ln R}, \quad (2)$$

where the proportion of each phenotype in a community is given by p_i with *R* denoting the maximum richness (here, 31 phenotypes). This provided a value between 0 to 1, with 0 indicating an uneven community dominated by a single phenotype and 1 indicating a community with equal proportions of all phenotypes represented.

For the Anderson and Kremer simulations, we also characterized phytoplankton community differences between parameterizations (Anderson and Kremer), as well as between time periods (control and climate change scenario) for each parameterization using Bray–Curtis dissimilarity. Here Bray–Curtis (BC) is calculated for each grid cell using the average PFT biomass (mg C m^{-3}) in the upper 240 m from each simulation (*a* and *b*) and each PFT (*i*), according to the following equation (Bray & Curtis, 1957):

$$BC_{ab} = \frac{\Sigma_i \left| PFT_i^a - PFT_i^b \right|}{\Sigma_i \left(PFT_i^a + PFT_i^b \right)}. \quad (3)$$

We used PFT biomass rather than phenotype biomass for this analysis to better capture the change in PFT composition that resulted from adjusting PFT thermal parameters within the model. We also did not include the Eppley simulations in this latter analysis after finding that the Eppley parameterizations produced phytoplankton community structures, which mostly lacked diatoms in the global ocean. Model output from these simulations are archived on the Harvard Dataverse (Anderson, 2023) and code to reproduce these analyses are archived at Zenodo (Anderson & Fronda, 2023).

3 | RESULTS

3.1 | Thermal trait evaluations

The Eppley parameterization method produced a single μ_{max} and Q_{10} that was generally lower than either the Kremer or Anderson methods (Table 1). When differentiating between PFTs, as in the Kremer and Anderson methods, the data suggest that diatoms exhibit the highest growth rates (e.g., μ_{max20}), while the diazotrophs and dinoflagellates have the lowest, consistent with previous findings (Anderson et al., 2021; Thomas et al., 2016). Following the Anderson method, the data indicate that cyanobacteria may exhibit the greatest response to temperature change, as evidenced by their high Q_{10} and steep curve slope (Figure 1c), while coccolithophores may exhibit the shallowest slope and lowest Q_{10}. This difference in slope signifies that the cyanobacteria would be able to increase their growth at a greater rate than the coccolithophores, making them increasingly strong competitors with each degree of temperature increase. This slope variability also results in different PFTs exhibiting growth dominance at different points along the temperature gradient, as evidenced by thermal dependency curve intersections within the Anderson parameterization (Figure 1c).

3.2 | Estimates of primary production

Differences in parameterized thermal traits between control simulations resulted in changes to community structure and biogeochemical processes. At low latitudes, each parameterization produced comparable estimates of total phytoplankton biomass and primary production in the upper 240 m (Figure 2). However, discrepancies emerged at mid and high latitudes (30–90° N/S), with the Eppley parametrization having higher biomass by an average of 25.5% when compared with the Kremer simulation, and 14.7% when compared with the Anderson simulation (Figure 2a; Figure S5a). These

differences in biomass resulted in subsequent variability in our primary production estimates (Figure 2b), as primary production in the Darwin model is calculated as a factor of biomass and growth rate (Dutkiewicz et al., 2020). At mid- and high latitudes, the Eppley parameterization led to primary production being higher by 24.5% when compared with Kremer, and 7.45% when compared with Anderson (Figure 2b; Figure S5b,d).

3.3 | Phytoplankton community structure

The phytoplankton community structures that resulted from each parameterization were more disparate than the bulk estimates of biomass and production in the control simulations. The Eppley simulation differed from both the Kremer and Anderson simulations substantially and was characterized by lower species richness (Figure 3a) and community evenness (Figure 3b), with significant differences at midlatitudes (30–60° N/S; one-way ANOVA, richness: $p < .001$, evenness: $p < .001$). Additionally, the PFT composition differed measurably between simulations, with the greatest variability in the Southern Ocean. There, the Eppley parameterizations produced a community dominated by dinoflagellates and coccolithophores, with roughly 8 times greater dinoflagellate biomass (mg C m^{-3}) at 50° S than either the Kremer (7.77×) or Anderson (8.12×) simulations (Figure 4). In comparison, the Kremer and Anderson simulations produced a phytoplankton community dominated by diatoms (Figure 3c), which were outcompeted globally in the Eppley simulations, as evidenced by their relatively low biomass (Figure 4a). Green algae also had narrower spatial distributions in the Eppley simulations, with the greatest biomass occurring 8–10° further equatorward in the Southern Hemisphere than in the Kremer or Anderson simulations (38° S vs. 48 or 46° S, respectively; Figure 4).

Between the Kremer and Anderson parametrizations, there were also distinct differences in community structure. For example, the global spatial distribution of cyanobacteria was 7.47% or 26 million km^2 smaller in the Anderson simulations than the Kremer simulations (Figure 4b,c), with cyanobacteria not extending South of 64° S. Conversely, the latitudinal extent of coccolithophores was 1.04% (3.5 million km^2) greater in the Anderson simulations, with coccolithophores exhibiting higher biomass in the Southern Ocean (Figure 4c). These differences produced a more even community in the Southern Ocean under the Anderson parameterization, but a less even community in the Arctic Ocean than the Kremer simulation (Figure 3b). Variability in community structure altered estimates of biogeochemical processes at high latitudes (Figure 5a,d,g). For example, the Anderson simulation estimated greater particulate inorganic carbon (PIC) by 0.55 mg C m^{-3} (9.83%) in the control scenario (Figure 5g).

3.4 | Community projections for the future

Using altered temperatures and physical forcing representative of the end of the century under a high emission scenario, we simulated climate change in our model ocean to understand how differences

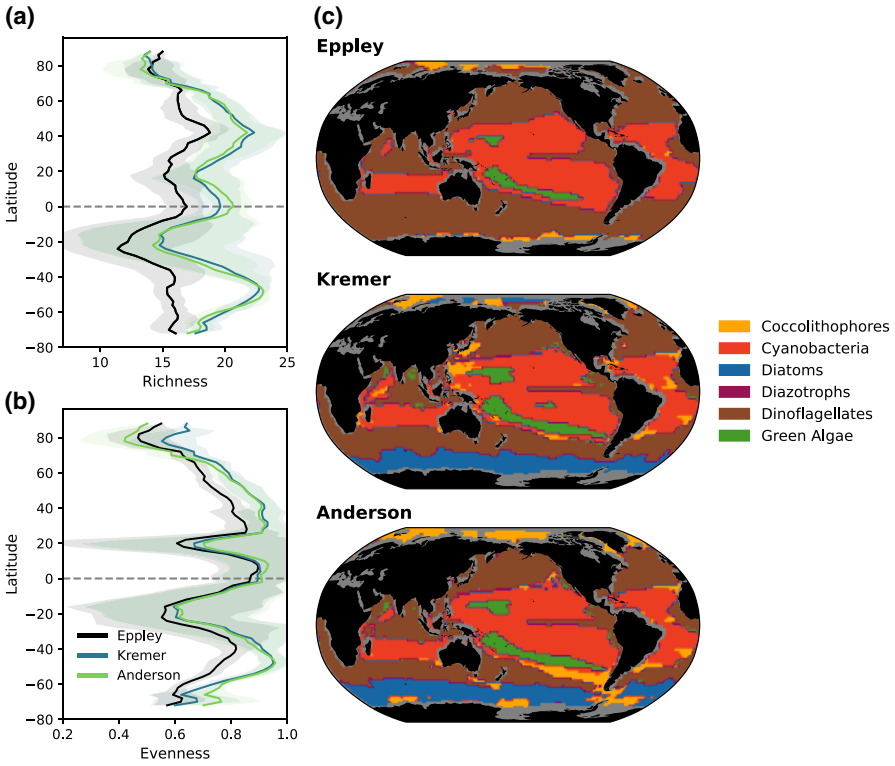

FIGURE 3 Zonal means (lines) and variation (±1 SD, shading) of phytoplankton community richness (a) and evenness (b) calculated from biomass in the upper 240 m in the control scenario averaged over the final 10 years (1870–1880). Only phytoplankton representing at least 0.001% of the total phytoplankton biomass were considered in calculations, following the methods of Barton et al. (2010) and Clayton et al. (2013). (c) The dominant Phytoplankton Functional Type at each location is indicated by colors (legend), with grey shading denoting unresolved or ice-covered regions within the model.

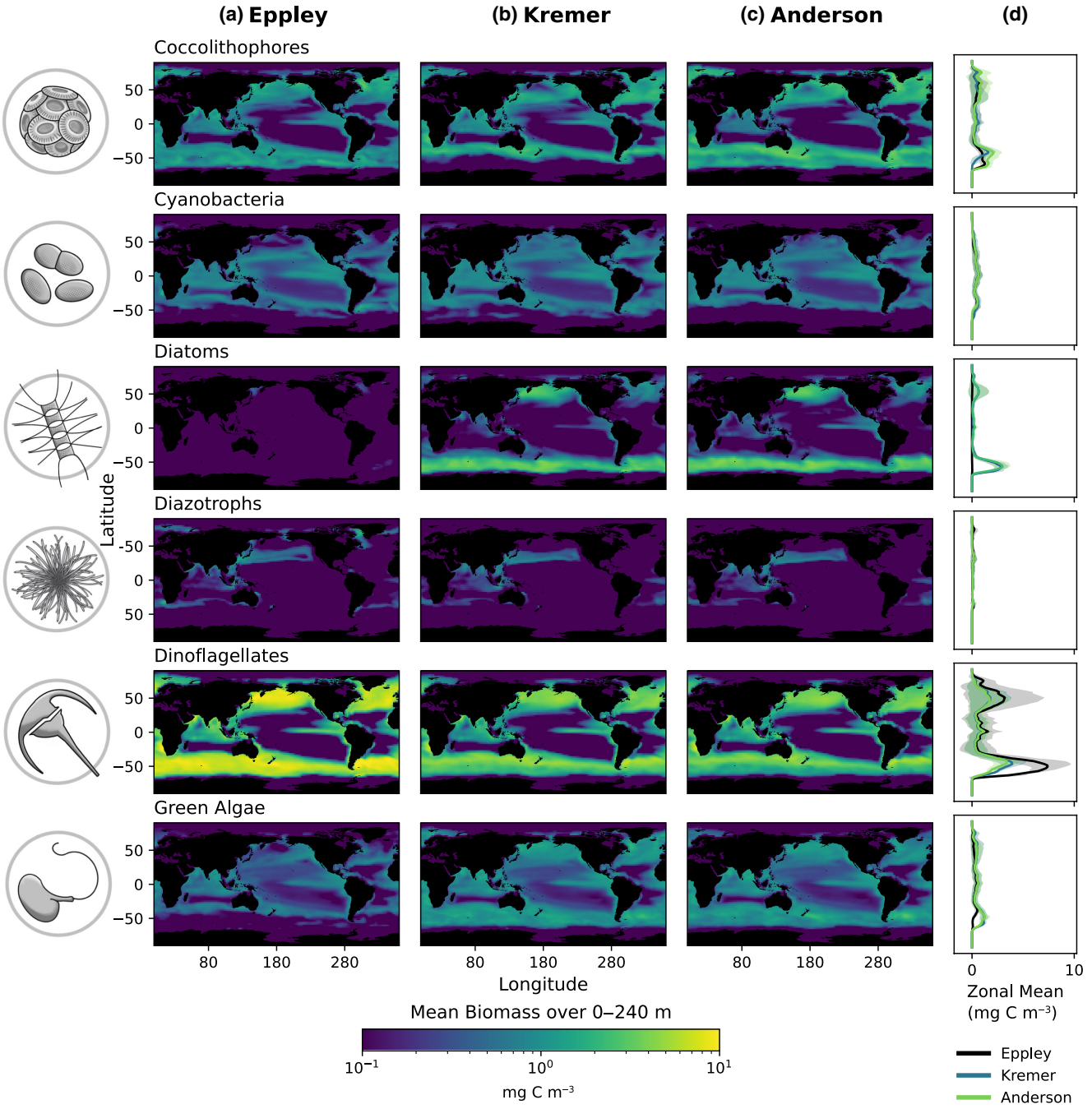

FIGURE 4 Mean biomass over the upper 240 m for each Phytoplankton Functional Type under each model parameterization (a–c) in the control simulation averaged over 10 years (1870–1880). Zonal mean and standard deviation are shown for each simulation (d).

in temperature-growth parameterizations might alter projections of phytoplankton communities and export in a future ocean. For this analysis, we focused on the Kremer and Anderson methods, as the Eppley method produced a phytoplankton community which unrealistically lacked diatoms globally (Figure 4a). We assessed differences in community structure using Bray–Curtis dissimilarity between the Kremer and Anderson methods using the average PFT biomass over the final 10 years of the control (1860–1880) and climate change simulation (2080–2100). Bray–Curtis dissimilarity considers both PFT presence/absence and biomass, and scores communities on a scale from 0 to 1, with '0' indicating identical communities and a '1' indicating completely different communities (no analogous PFTs). At low latitudes, the Kremer and Anderson parameterizations predicted similar alterations to the phytoplankton community with climate change (low Bray–Curtis dissimilarity; Figure 6a). However, the phytoplankton communities in the control and climate change scenarios varied substantially between the Kremer and Anderson simulations (Figure 6b) and were greater than within each simulation due to climate change (1860 and 2100 physical conditions, Figure 6a).

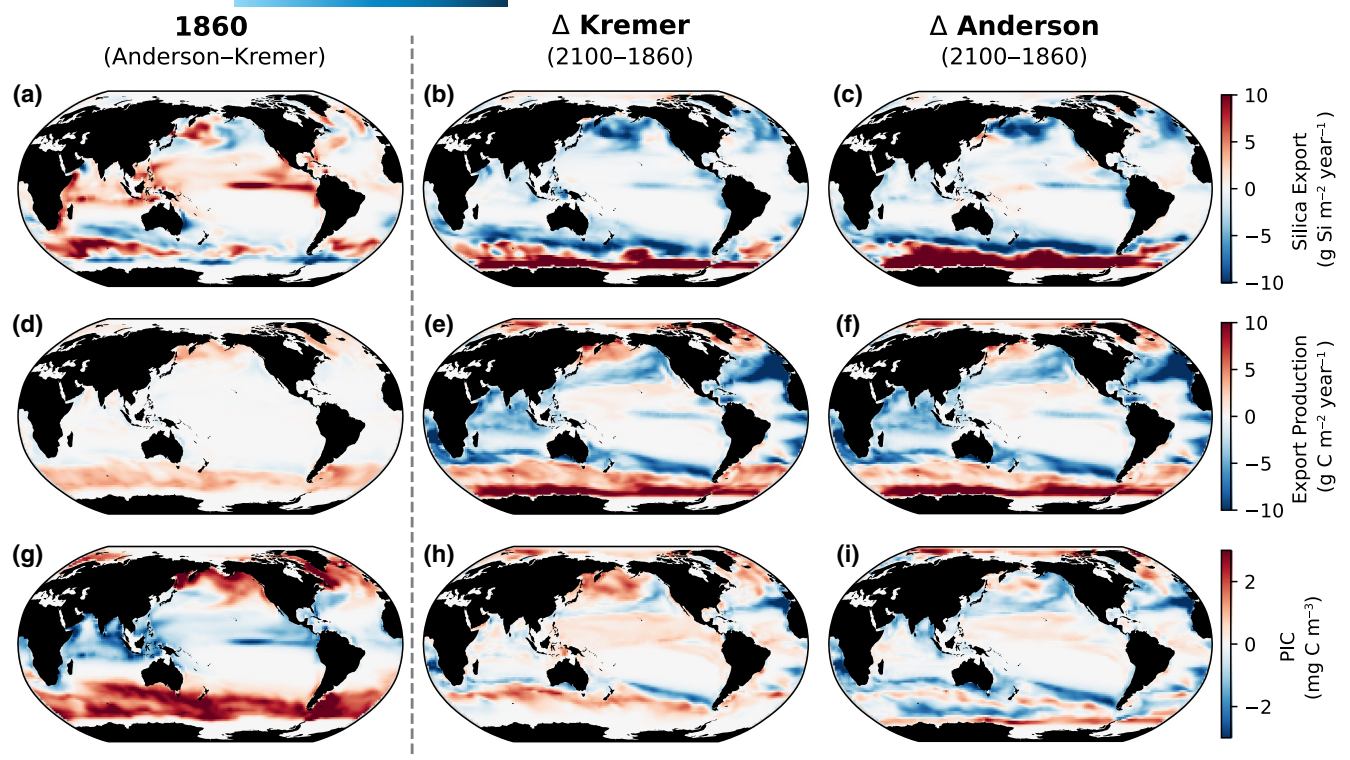

FIGURE 5 Difference in silica export (a–c; g Si m^{-2} $year^{-1}$), export production (d–f; g C m^{-2} $year^{-1}$), and particulate inorganic carbon (PIC; g–i; mg C m^{-3}) at 115 m between models, averaged over the final 10 years of each simulation. The difference between the Anderson and Kremer parameterizations (Anderson–Kremer) in the control [mean (1870–1880)] is shown in (a, d, g) and the change in export processes with climate change [mean (2090–2100) – mean (1870–1880)] is characterized for Kremer (b, e, h) and Anderson (c, f, i).

These disparities in phytoplankton communities were primarily driven by differences in PFT proportions (evenness). For example, in the control scenario, evenness varied between the Kremer and Anderson simulations at high latitudes (Figure 3b) because of differences in PFT biomass (Figure 4), especially for coccolithophores and cyanobacteria. The coccolithophores also exhibited the greatest differences in biomass change (1860–2100) between simulations, with biomass change ~20× less with the Anderson parameterizations at Southern mid-latitudes than in the Kremer parameterizations (Figure 7a; Figure S6), due primarily to the coccolithophores having the lowest Q_{10} in the Anderson simulation, relative to the other PFTs. This resulted in large differences in our estimates of calcium carbonate (PIC) alterations with climate change, with the Kremer simulation predicting increases in PIC and the Anderson method predicting decreases in PIC at the poles (Figure 5h,i, respectively). Though the community differences were large between the Anderson and Kremer scenarios, the directionality of biomass change, with PFT biomass either increasing or decreasing between the control and 2100 environment, agreed between simulations in most regions (Figure 7). Notably, both parameterizations suggest a decrease in cyanobacteria in the gyres (Figure 7b; Figure S6), but an increase at higher latitudes, while diatoms are suggested to decrease almost everywhere (except in the Southern Ocean; Figure 7c). This consensus in biomass change also resulted in a general agreement between simulations for how export production might be altered by 2100 (Figure 5).

4 | DISCUSSION

Over 50 years ago, Eppley first documented the response of phytoplankton growth to changes in temperature (Eppley, 1972). The canonical Q_{10}=1.88 has been, and continues to be, used in many models, including those providing estimates of the impact of climate change on the ocean's biogeochemistry (Bopp et al., 2013; Laufkotter et al., 2015). However, as these models added even modest increases in plankton diversity (e.g., two rather than one PFT), it became clear that uniform traits were unrealistic. Most models now include at least a fast-growing diatom and a slower growing smaller phytoplankton with varied μ_{max} (similar to the Kremer method), or implicit functions like calcification, though few include mixotrophy (Laufkotter et al., 2015). Despite this added diversity, the method of choosing Q_{10} and μ_{max} varies from model to model with most models electing to apply a single Q_{10} universally among PFTs. However, recent observations suggest that PFTs exhibit unique responses to temperature (Anderson et al., 2021; Kremer et al., 2017) and employing a single universal thermal trait, as in the Eppley method, may result in coarse estimations of ecological processes in the global ocean. Using a single empirical dataset, we evaluated three methods of parameterizing the Q_{10} and μ_{max} to provide an outline of the strengths and limitations of each method. Our robust framework allowed us to compare the ecological and biogeochemical consequences of different thermal response trait parameterizations, which will help strengthen the predictive capacity of biogeochemical and ecosystem models.

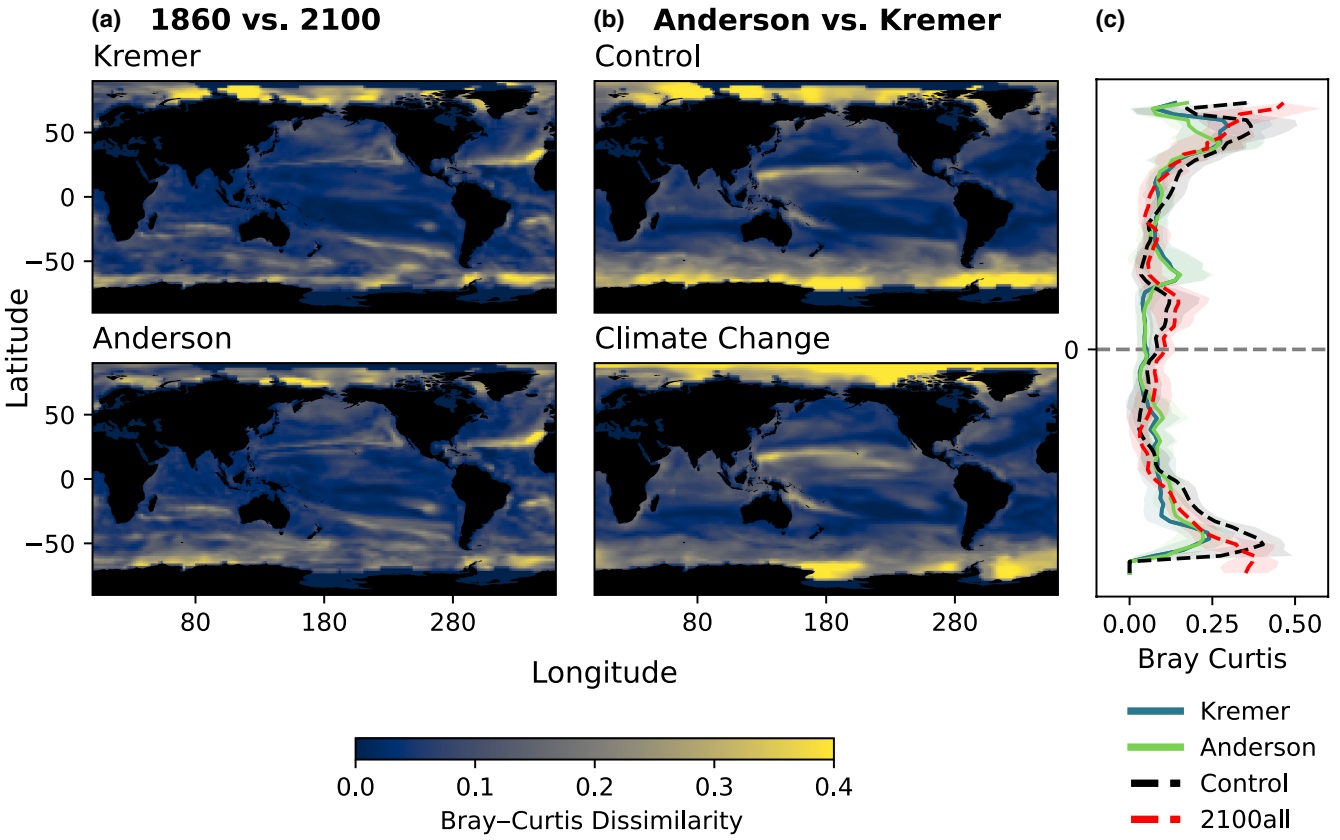

FIGURE 6 Bray–Curtis dissimilarity from 1860 to 2100 (a) for the Kremer and Anderson parameterizations under a climate change scenario (e.g., nutrient concentrations, circulation etc. changing), versus a community comparison between models at each time point (b; 1870–1880 (control) or 2090–2100 (climate change)). A '0' indicates no change in phytoplankton community and a '1' indicates a community with no analogous Phytoplankton Functional Types (PFTs). Zonal means (lines) and standard deviations (shading) are also shown (c). Only PFTs representing at least 0.001% of the total phytoplankton biomass were considered.

4.1 | Simulating diverse phytoplankton communities

One of the principal findings of our control simulations was the difference in community structures produced by each parameterization. The Eppley formulation in particular produced an ocean almost entirely absent of diatoms. This differs significantly from satellite-based estimations of phytoplankton community structure, which characterize diatoms as the dominant PFT in the Southern Ocean during austral summer (Figure S7a; Alvain et al., 2008; Xi et al., 2020), as well as empirical observations which note considerable diatom biomass throughout the world's oceans, and especially in the Southern Ocean (Figure S8; Leblanc et al., 2012). The absence of diatoms in the Eppley simulation was due in part to the way in which growth rates were parameterized, with all PFTs characterized by the same μ_{max}, contradicting evidence that diatoms can be strong competitors in high nutrient regimes and have some of the fastest phytoplankton growth rates (Alexander et al., 2015; Anderson et al., 2021; Tang, 1995). Global biogeochemical and plankton community models have generally parameterized higher growth rates for diatoms based on these empirical observations of greater nutrient uptake (Aumont & Bopp, 2006; Follows et al., 2007; Gregg & Casey, 2007; Negrete-García et al., 2022; Stock et al., 2014) and are often able to reproduce substantial diatom communities in the Southern Ocean (Bopp et al., 2005). However, rarely is the μ_{max} also temperature-dependent, with some exceptions (Shigemitsu et al., 2012), or evaluated using as rigorous of a methodology as provided here. We find that without employing a higher μ_{max}, and with diatoms' higher nutrient requirements (due to their larger size), diatoms are outcompeted in the simulated global ocean. In the Eppley simulation, dinoflagellates were the main competitor of the diatoms and excelled given their ability to supplement their nutrient requirements with grazing (mixotrophy). These results highlight the limitations of parameterizing ecosystem models strictly according to the Eppley method, as simulations produced phytoplankton community structures that contradict observations from the natural world (Alvain et al., 2008; Leblanc et al., 2012; Soppa et al., 2014; Xi et al., 2020).

While many ocean plankton community models have included different μ_{max} between PFTs, they generally utilize a single Q_{10} (Bopp et al., 2013; Laufkotter et al., 2015). As such, most models (Bopp et al., 2013; Follows et al., 2007; Laufkotter et al., 2015) follow an approach closer to our Kremer method, with some exceptions (Buitenhuis et al., 2013). However, the choice of different Q_{10}'s between PFTs has typically not been rigorously differentiated for many

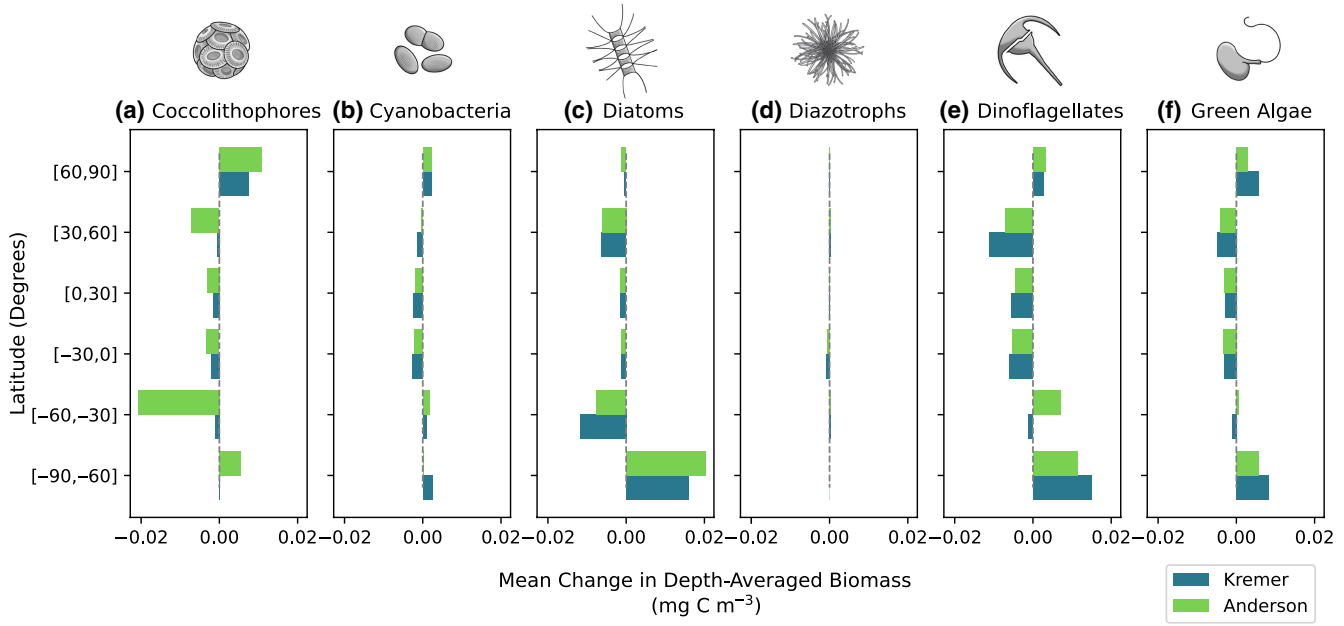

FIGURE 7 Average change in biomass for each Phytoplankton Functional Type (PFT; a–f), over the upper 240 m between the final 10 years of the control (1870–1880) and climate change scenario (2090–2100) for the Kremer (blue) and Anderson (green) parameterizations. PFT changes over time were binned into high (60–90°), mid (30–60°), and low (0–30°) latitudes.

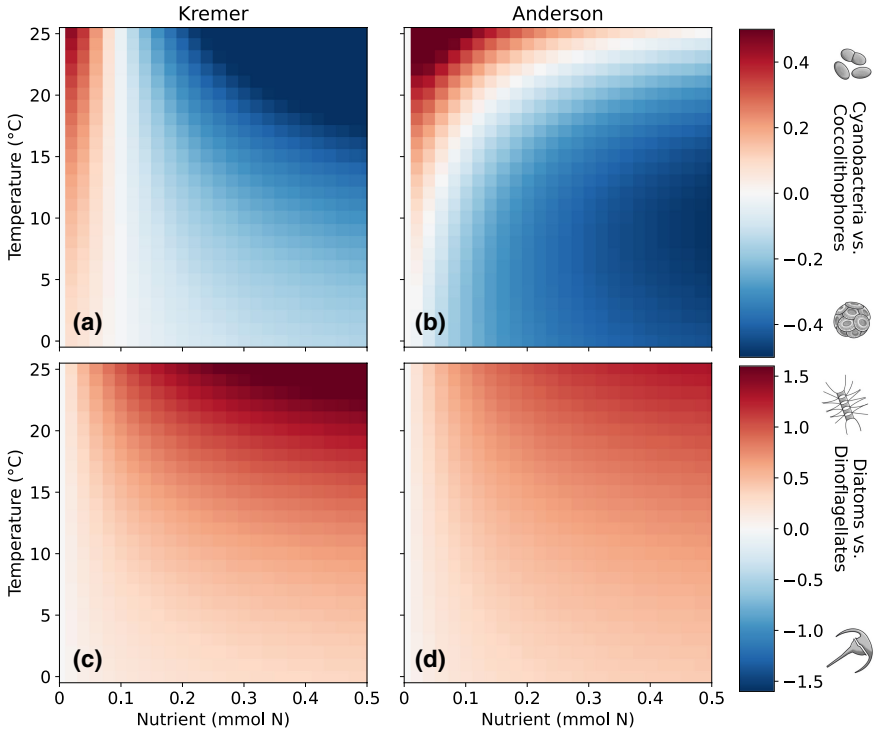

FIGURE 8 Difference in growth rate (per day) between cyanobacteria and coccolithophores (a, b) and diatoms and dinoflagellates (c, d) in a simplified Kremer (a, c) or Anderson (b, d) model where growth depends only on temperature and nutrient availability (Equation 4). Phytoplankton Functional Type (PFT) icons indicate which conditions lead to one PFT exhibiting a higher growth rate over another (red or blue).

PFTs, using a single coherent dataset, and is not normally based on thermal growth curves as is done here. By estimating both the μ_{max} and the Q_{10} in a consistent manner, we were able to characterize each PFT's thermal dependency and compare parameterization methods. From this analysis, we found that parameterizing PFTs with a unique μ_{max} while holding the Q_{10} constant (Kremer) or allowing it to vary (Anderson), better simulated natural phytoplankton assemblages than the Eppley method. In lower latitudes, the two parameterizations had similar community structures. In these regions, smaller phytoplankton adapted to low nutrient conditions dominate, as nutrient affinity is a more important factor in determining competitive ability than differences in Q_{10}. But poleward, there are notable differences between these two parameterizations. For instance, the poleward extent of cyanobacteria was reduced in the Anderson simulation, better reflecting global cyanobacteria distributions. Abundance patterns of the cyanobacteria *Synechococcus*

and *Prochlorococcus*, collected via cruise transects, often characterize a clear drop in cyanobacteria density approaching the poles (Flombaum et al., 2013; Follett et al., 2022), resembling that of the Anderson simulation. This decrease in abundance can partially be explained via the increase in shared predation of cyanobacteria and heterotrophic bacteria at higher latitudes, which are similar in size (Follett et al., 2022). However, as our iteration of the Darwin model includes heterotrophic bacteria in both the Kremer and Anderson simulations, we can also hypothesize that the varied temperature coefficients (Q_{10}) in the Anderson parameterization contribute to the observed differences in cyanobacteria biomass. In particular, the steeper Q_{10} for cyanobacteria reduces their competitive ability at low temperatures.

Coccolithophores were another PFT whose geographical range varied between control simulations, with a greater poleward extent exhibited in the Anderson simulation. Coccolithophores are calcifying phytoplankton that comprise the Southern Ocean Great Calcite Belt which extends as far South as 65° (Holligan et al., 2010). The calcium carbonate (PIC) that they produce is visible via satellite and is at its highest concentration at high latitudes (Mitchell et al., 2017). Though in-situ observations are sparse for the coccolithophores (Figure S8), they are thought to contribute considerably to total annual production in the Southern Ocean (Nissen et al., 2018), again supporting coccolithophore presence in polar regions. This distribution pattern is captured in the Darwin model only when the coccolithophores are parameterized with a lower Q_{10}, supporting the use of the Anderson formulation in high latitude ecosystem models.

To further demonstrate and highlight the impact of these varied Q_{10}'s on PFT competitive abilities, we provide a simplified illustrative example of the temperature-nutrient growth relationship under the Kremer and Anderson parameterizations (Figure 8). Here, we evaluate the growth of just two representative phenotypes (Figure S1), the fastest grower from each PFT (Figure S4, Methods). Growth (μ) is dependent only on temperature (T) and nitrogen (N; the full model includes other elements as well as a light-dependency) according to the following equation (expanded from Equation 1), where the maximum growth at $T=0$°C ($\mu_{\max[0]}$) scales with temperature at a rate of b and nutrient concentration [N] based on a half-saturation constant of nitrate K_{NO_3} (Table S3):

$$\mu_{[T,N]} = \mu_{\max[0]} \cdot e^{(b \cdot T)} \cdot \frac{[N]}{[N] + K_{NO_3}}. \quad (4)$$

We show the differences in growth rates for PFTs that have very different Q_{10}'s, cyanobacteria and coccolithophores (Figure 8a,b), and for PFTs that have similar Q_{10}'s, diatoms and dinoflagellates (Figure 8c,d), both when the Q_{10} is held constant (Kremer) and when it is differentiated (Anderson). When PFTs have similar Q_{10}'s, we expect similar competitive abilities as we transition across environmental gradients, regardless of how the Q_{10}'s are parameterized (Figure 8c,d). However, PFTs with large differences in their Q_{10} are significantly impacted by Q_{10} parameterization. In the Kremer simulation, cyanobacteria only outcompete coccolithophores in low-nutrient environments (Figure 8a), whereas in the Anderson simulation, this competitive relationship is more nuanced, with cyanobacteria growing faster in both nutrient-limited systems and high temperature regimes, and coccolithophores exceling in nutrient-replete, colder environments (Figure 8b). By parameterizing PFTs with unique Q_{10}'s, we are thus adjusting how phytoplankton compete across the world's oceans.

4.2 | Projecting into the future

These differences in modeled competitive abilities extended into the future with climate change. Our results demonstrated that model parameterization substantially impacts the starting phytoplankton community assemblage, which is then carried forward in climate change scenarios, consequently impacting estimates of export processes. Though some studies have examined phytoplankton diversity and PFT turnover with climate change (e.g., Henson et al., 2021), few have estimated how the biomass of specific PFTs might be altered in the future (Le Quéré et al., 2005) and that has contributed to a lack of consensus for each PFT's relative contributions to primary (Laufkotter et al., 2015) and secondary production (Dutkiewicz et al., 2021).

Between the Kremer and Anderson methods, there was consensus regarding the directionality of change (either positive or negative) expected for each PFT at each latitude with climate change (Figure 7). Both parameterizations showed the expansion of the oligotrophic gyres (Figure S9) and the dominance of smaller phytoplankton (Figure S10) predicted by many previous modelling studies (e.g., Bopp et al., 2005; Marinov et al., 2010). They also both predicted an increase in diatom abundance in the Southern Ocean (Figure 7c), which would increase the Southern Ocean's role as the 'silicon trap', or the region of the greatest silica export (Holzer et al., 2014), which may be partially due to light limitation being alleviated as ice extent is reduced. These similar projected changes in PFT biomass led to parallel projections for export production (Figure 5e,f). However, there was disagreement on the magnitude of biomass change to be expected for each PFT (Figure 7), which lead to discrepancies in estimates of other export processes, like PIC (Figure 5h,i). For example, in the Anderson simulation (Figure 5i), PIC is projected to decrease due to a reduction in coccolithophore biomass. Observations in the natural world suggest this may already be occurring, with documented declines in the poleward extent of coccolithophore blooms in recent years, attributed to increases in sea-surface temperature (Uz et al., 2013). Although on a different timeframe, the Anderson simulation similarly finds this decline in coccolithophore biomass which is not captured in the Kremer simulations.

To explore the differences in PFTs further, we ran a warming-only simulation, in which nutrient and physical dynamics were as

for the control, but temperature changed. With warming alone, the phytoplankton communities under the Kremer parameterization remained relatively constant through time (Figure S11), whereas the communities in the Anderson simulations exhibited large changes, especially at the poles. Returning to our illustrative example (Figure 8), this would be similar to moving along the temperature axis only, rather than dynamically in temperature/nutrient space, as would be expected in a full climate change scenario. This suggests that by applying a Q_{10} universally, as in the Kremer method, PFT competitive abilities become largely temperature independent, masking important inter-group dynamics and overturn.

In summary, we found that using the same μ_{max} and Q_{10} across all modeled PFTs (Eppley) did not lead to a realistic phytoplankton community structure, but resulted in estimates of primary production that were comparable to Kremer and Anderson in lower latitudes, though not at higher. Our findings also demonstrated how the phytoplankton assemblage is impacted by varied Q_{10}'s, especially at higher latitudes. At lower latitudes, nutrient limitation was often a more important control on community structure but with higher nutrient concentrations further poleward, the temperature effect became more important. Thus, we found that the Kremer (same Q_{10}) and Anderson (unique Q_{10}) methods produced similar communities at low latitudes, but the Q_{10} parameterization substantially impacted each PFTs competitive abilities at higher latitudes. This was most pronounced with climate change, as warming led to substantial changes in phytoplankton diversity with the Anderson but not the Kremer parameterization. Though observational data is not currently sufficient to discern whether the Kremer or Anderson method results in a more realistic control phytoplankton community (Figure S8), the lack of diversity change in the Kremer simulations under ocean warming (Figure S11) suggests that the Anderson method would be preferential when examining future high latitude communities, even though it requires greater model complexity, as temperature-related competition is likely to impact phytoplankton community structure with climate change (Table 2).

TABLE 2 The growth parameters which significantly impacted estimates of biogeochemical processes at each latitude. Listed in parentheses are the methods that differentiated between Phytoplankton Functional Types for these parameters (K: Kremer; A: Anderson), potentially increasing model realism. Where we state 'Ambiguous' we indicate that results were comparable between all methods.

	Low latitudes	High latitudes
Primary production	Ambiguous (all comparable)	μ_{max} (K, A)
Community structure	μ_{max} (K, A)	μ_{max} & Q_{10} (A)
Export processes	μ_{max} (K, A)	μ_{max} & Q_{10} (A)
Climate change	μ_{max} & Q_{10} (A)	μ_{max} & Q_{10} (A)

4.3 | Study limitations

The MIT biogeochemistry and ecosystem model, Darwin, resolves PFTs at finer physiological scale than most ecological models. However, like all models, it cannot capture all the complexity we know to exist in the natural world. Given the model's current parameterization, the temperature dependence of nutrient uptake and growth are assumed the same. Yet, some research on diatoms suggests that nutrient uptake processes may each have their own optimal temperature (Baker et al., 2016). Similarly, nutrient availability may also alter the thermal response, with the μ_{max}, Q_{10}, and thermal optimum, the temperature that produces the greatest growth, shifting based on nutrient availability (Marañón et al., 2018). Light availability may have a similar effect, altering the temperature sensitivity of phytoplankton (Edwards et al., 2016). For these relationships to be characterized and accounted for in ecosystem models, more laboratory experiments across a diverse range and concentration of environmental drivers and using multiple PFTs are needed (Collins et al., 2022).

On a broader scale, there is also some debate about whether the exponential curve, first described by Eppley to portray the μ_{max} relationship with temperature and characterize the Q_{10} (Eppley, 1972), accurately depicts the phytoplankton response to temperature at the thermal extremes (low and high temperatures). Some data suggest that the exponential temperature-growth relationship may break down at higher temperatures (Anderson et al., 2021), potentially indicating a limit to the thermal dependency. This may be caused by thermodynamic constraints, like enzyme structure and membrane fluidity, both of which have thermal limits (Willmer et al., 2004) leading to negatively skewed thermal performance curves in individual phytoplankters (a rapid decline in growth above the thermal optima, Thomas et al., 2012). Thus, fitting exponential curves to thermally constrained growth rates may not be representative of the temperature-growth relationship and could lower the resulting Q_{10}. While the goal of this study was to evaluate the parameterization of the Q_{10} and not the exponential relationship from which it is derived, defining a new function that would better describe the thermal dependency remains an active area of research worth pursuing to further improve our ecosystem models.

At last this modeling study is highly simplified for demonstrative purposes. Though we aimed to characterize the effect of thermal traits on phytoplankton community composition, we could not include all of the features that delineate PFTs, such as cell shape (Margalef, 1978; Naselli-Flores et al., 2021), nor could we capture all of the diversity, complexity of organismal interactions, potential for trait evolution, or transient processes which may have impacted competition and therefore community structure historically or which will alter communities with climate change (Bishop et al., 2022; Padfield et al., 2016). Additionally, due to the model's global scale and course resolution, plankton are advected and mixed within the flow field, but smaller scale features (e.g., eddies, turbulence) are not explicitly included. Instead, we designed this experiment to explore the impacts of different thermal trait parameterizations in an

idealized, model setting. Though we have begun to disentangle the value of increased PFT thermal trait differentiation in ocean-only biogeochemical models, comparing modeled PFT distribution from each simulation with empirical knowledge and observations (satellite and in situ sampling), we cannot explicitly state that the Kremer method produces more realistic phytoplankton communities than the Anderson method, or vice versa, as we do not have the observational data and global coverage needed to support such a conclusion. We also cannot validate each simulation's primary production estimates, as satellite derived estimates of net primary production are highly variable depending on the algorithms employed, varying more than the differences between our model experiments (Stock, 2019). However, we can highlight how each method may lead to different understandings of certain PFTs or regions (e.g., high latitudes) or cause predictions for a future ocean to vary so widely between Earth system models (Kwiatkowski et al., 2020; Laufkotter et al., 2015).

5 | CONCLUSIONS

This work illustrated the impacts of phytoplankton thermal trait parameterization on estimates of phytoplankton community structure and biogeochemical cycling in a historical and climate change scenario. Several studies have estimated the Q_{10} from thermal growth data obtained from laboratory studies (Anderson et al., 2021; Bissinger et al., 2008; Eppley, 1972; Kremer et al., 2017); however, our study is unique in that it used a single empirically derived temperature-growth dataset, with differing assumptions about whether PFTs should be analyzed separately, to more consistently calculate the Q_{10} and μ_{max} (Table 1). We then investigated how these different assumptions impacted community structure, competition, and productivity in a global ecosystem model. The Eppley method of assuming all PFTs have the same Q_{10} and μ_{max} provided productivity estimates that matched observations in low latitudes, but hindered diatoms, eliminating them from the global ocean. For studies interested in diversity, food web structures, or export processes, both the Kremer and Anderson methods should be preferentially employed for their higher capacity to recreate natural community structures. Between these methods, the Anderson formulation captures variability in the temperature coefficients (Q_{10}) of each PFT, resulting in key differences in competition and export, especially at high latitudes, while the Kremer method provides a simpler approach which produces comparable phytoplankton communities at low latitudes, where nutrient limitation plays a larger role in determining which PFTs can survive. Though the Kremer and Anderson methods had significant differences in historical community structure, they both showed similar directionality of PFT biomass change in the future ocean. However, there were important differences in the magnitudes of these changes, especially in key PFTs and along the edges of expanding gyre boundaries.

This assessment serves as an illustrative guide for parameterizing phytoplankton ecosystem models, showcasing the strengths and weaknesses of three key methodologies. This study also emphasizes how the parameterization of the μ_{max} and Q_{10} can alter our understanding of phytoplankton community structure, with a steeper or shallower thermal dependency curve impacting the range of temperatures and regions where one PFT may outcompete another, thus altering projections for the future in Earth system models.

AUTHOR CONTRIBUTIONS

Stephanie I. Anderson: Conceptualization; data curation; formal analysis; funding acquisition; methodology; visualization; writing – original draft; writing – review and editing. **Clara Fronda:** Conceptualization; formal analysis; funding acquisition; methodology; visualization; writing – original draft; writing – review and editing. **Andrew D. Barton:** Conceptualization; formal analysis; writing – review and editing. **Sophie Clayton:** Conceptualization; formal analysis; writing – review and editing. **Tatiana A. Rynearson:** Conceptualization; formal analysis; funding acquisition; writing – review and editing. **Stephanie Dutkiewicz:** Conceptualization; data curation; formal analysis; funding acquisition; methodology; resources; supervision; visualization; writing – original draft; writing – review and editing.

ACKNOWLEDGEMENTS

This work was supported by a grant from the Simons Foundation (874777, SIA). This work was also supported in part by the Simons Collaboration on Computational Biogeochemical Modeling of Marine Ecosystem/CBIOMES (Grant ID: 549931FY22, SD, CF) and by The National Science Foundation award #1638834 (to TAR).

CONFLICT OF INTEREST STATEMENT

The authors declare no conflict of interest.

DATA AVAILABILITY STATEMENT

The Darwin ecosystem model used in this study is available through https://github.com/darwinproject/darwin3, and the physical model is available through https://mitgcm.org. Outputs from model simulations are archived on the Harvard Dataverse (Anderson, 2023). Code to reproduce these analyses are available on GitHub (https://github.com/sianderson/Thermal_trait_parameterization) and archived at Zenodo (Anderson & Fronda, 2023).

ORCID

Stephanie I. Anderson https://orcid.org/0000-0002-2458-0922
Andrew D. Barton https://orcid.org/0000-0002-6480-4433
Sophie Clayton https://orcid.org/0000-0001-7473-4873
Tatiana A. Rynearson https://orcid.org/0000-0003-2951-0066
Stephanie Dutkiewicz https://orcid.org/0000-0002-0380-9679

REFERENCES

Alexander, H., Rouco, M., Haley, S., Wilson, S., Karl, D., & Dyhrman, S. (2015). Functional group-specific traits drive phytoplankton

dynamics in the oligotrophic ocean. *Proceedings of the National Academy of Sciences of the United States of America*, *112*(44), E5972–E5979. https://doi.org/10.1073/pnas.1518165112

Alvain, S., Moulin, C., Dandonneau, Y., & Loisel, H. (2008). Seasonal distribution and succession of dominant phytoplankton groups in the global ocean: A satellite view. *Global Biogeochemical Cycles*, *22*(3), 1–15. https://doi.org/10.1029/2007GB003154

Anderson, S. I. (2023). *Thermal_Trait_Parameterization*. Harvard Dataverse. https://doi.org/10.7910/DVN/6TLL8Z

Anderson, S. I., Barton, A. D., Clayton, S., Dutkiewicz, S., & Rynearson, T. (2021). Marine Phytoplankton Functional Types exhibit diverse responses to thermal change. *Nature Communications*, *12*(6413), 1–9. https://doi.org/10.1038/s41467-021-26651-8

Anderson, S. I., & Fronda, C. (2023). Sianderson/thermal_trait_parameterization: Phytoplankton thermal trait parameterization alters community structure and biogeochemical processes in a modeled ocean. *Zenodo*. https://doi.org/10.5281/zenodo.10223059

Aumont, O., & Bopp, L. (2006). Globalizing results from ocean in situ iron fertilization studies. *Global Biogeochemical Cycles*, *20*(2), 1–15. https://doi.org/10.1029/2005GB002591

Baker, K. G., Robinson, C. M., Radford, D. T., McInnes, A. S., Evenhuis, C., & Doblin, M. A. (2016). Thermal performance curves of functional traits aid understanding of thermally induced changes in diatom-mediated biogeochemical fluxes. *Frontiers in Marine Science*, *3*(April), 1–14. https://doi.org/10.3389/fmars.2016.00044

Barton, A., Dutkiewicz, S., Flierl, G., Bragg, J., & Follows, M. (2010). Patterns of diversity in marine phytoplankton. *Science*, *372*(5972), 1509–1511. https://doi.org/10.1126/science.1184961

Bishop, I. W., Anderson, S. I., Collins, S., & Rynearson, T. A. (2022). Thermal trait variation may buffer Southern Ocean phytoplankton from anthropogenic warming. *Global Change Biology*, *28*(19), 5755–5767. https://doi.org/10.1111/gcb.16329

Bissinger, J. E., Montagnes, D. J. S., Sharples, J., & Atkinson, D. (2008). Predicting marine phytoplankton maximum growth rates from temperature: Improving on the Eppley curve using quantile regression. *Limnology and Oceanography*, *53*(2), 487–493. https://doi.org/10.4319/lo.2008.53.2.0487

Bopp, L., Aumont, O., Cadule, P., Alvain, S., & Gehlen, M. (2005). Response of diatoms distribution to global warming and potential implications: A global model study—Art. no. L19606. *Geophysical Research Letters*, *32*(19), 19606. https://doi.org/10.1029/2005GL023653

Bopp, L., Resplandy, L., Orr, J. C., Doney, S. C., Dunne, J. P., Gehlen, M., Halloran, P., Heinze, C., Ilyina, T., Séférian, R., Tjiputra, J., & Vichi, M. (2013). Multiple stressors of ocean ecosystems in the 21st century: Projections with CMIP5 models. *Biogeosciences*, *10*(10), 6225–6245. https://doi.org/10.5194/bg-10-6225-2013

Bray, J. R., & Curtis, J. T. (1957). An ordination of the upland forest communities of southern Wisconsin. *Ecological Monographs*, *27*(4), 325–349. https://doi.org/10.2307/1942268

Buitenhuis, E. T., Hashioka, T., & Quéré, C. L. (2013). Combined constraints on global ocean primary production using observations and models. *Global Biogeochemical Cycles*, *27*(3), 847–858. https://doi.org/10.1002/gbc.20074

Cael, B. B., Dutkiewicz, S., & Henson, S. (2021). Abrupt shifts in 21st-century plankton communities. *Science Advances*, *7*, eabf8593. https://doi.org/10.1126/sciadv.abf8593

Clayton, S., Dutkiewicz, S., Jahn, O., & Follows, M. J. (2013). Dispersal, eddies, and the diversity of marine phytoplankton. *Limnology and Oceanography: Fluids and Environments*, *3*(1), 182–197. https://doi.org/10.1215/21573689-2373515

Collins, S., Whittaker, H., & Thomas, M. K. (2022). The need for unrealistic experiments in global change biology. *Current Opinion in Microbiology*, *68*, 102151. https://doi.org/10.1016/j.mib.2022.102151

Dutkiewicz, S., Boyd, P. W., & Riebesell, U. (2021). Exploring biogeochemical and ecological redundancy in phytoplankton communities in the global ocean. *Global Change Biology*, *27*(6), 1196–1213. https://doi.org/10.1111/gcb.15493

Dutkiewicz, S., Cermeno, P., Jahn, O., Follows, M. J., Hickman, A. E., Taniguchi, D. A. A., & Ward, B. A. (2020). Dimensions of marine phytoplankton diversity. *Biogeosciences Discussions*, *17*(3), 609–634. https://doi.org/10.5194/bg-2019-311

Dutkiewicz, S., Hickman, A. E., Jahn, O., Gregg, W. W., Mouw, C. B., & Follows, M. J. (2015). Capturing optically important constituents and properties in a marine biogeochemical and ecosystem model. *Biogeosciences*, *12*(14), 4447–4481. https://doi.org/10.5194/bg-12-4447-2015

Dutkiewicz, S., Hickman, A. E., Jahn, O., Henson, S., Beaulieu, C., & Monier, E. (2019). Ocean colour signature of climate change. *Nature Communications*, *10*, 578. https://doi.org/10.1038/s41467-019-08457-x

Dutkiewicz, S., Morris, J. J., Follows, M. J., Scott, J., Levitan, O., Dyhrman, S. T., & Berman-Frank, I. (2015). Impact of ocean acidification on the structure of future phytoplankton communities. *Nature Climate Change*, *5*(11), 1002–1006. https://doi.org/10.1038/nclimate2722

Dutkiewicz, S., Scott, J. R., & Follows, M. J. (2013). Winners and losers: Ecological and biogeochemical changes in a warming ocean. *Global Biogeochemical Cycles*, *27*(2), 463–477. https://doi.org/10.1002/gbc.20042

Edwards, K. F., Thomas, M. K., Klausmeier, C. A., & Litchman, E. (2016). Phytoplankton growth and the interaction of light and temperature: A synthesis at the species and community level. *Limnology and Oceanography*, *61*(4), 1232–1244. https://doi.org/10.1002/lno.10282

Eppley, R. W. (1972). Temperature and phytoplankton growth in the sea. *Fishery Bulletin*, *70*, 1063–1085.

Falkowski, P. G., Barber, R. T., & Smetacek, V. (1998). Biogeochemical controls and feedbacks on ocean primary production. *Science*, *281*(1998), 200–206. https://doi.org/10.1126/science.281.5374.200

Falkowski, P. G., Laws, E. A., Barber, R. T., & Murray, J. W. (2003). Phytoplankton and their role in primary, new, and export production. In M. J. R. Fasham (Ed.), *Ocean biogeochemistry. Global change—The IGBP series (closed)*. Springer. https://doi.org/10.1007/978-3-642-55844-3_5

Flombaum, P., Gallegos, J. L., Gordillo, R. A., Rincón, J., Zabala, L. L., Jiao, N., Karl, D. M., Li, W. K., Lomas, M. W., Veneziano, D., Vera, C. S., Vrugt, J. A., & Martiny, A. C. (2013). Present and future global distributions of the marine Cyanobacteria *Prochlorococcus* and *Synechococcus*. *Proceedings of the National Academy of Sciences of the United States of America*, *110*(24), 9824–9829. https://doi.org/10.1073/pnas.1307701110

Follett, C. L., Dutkiewicz, S., Ribalet, F., Zakem, E., Caron, D., Armbrust, E. V., & Follows, M. J. (2022). Trophic interactions with heterotrophic bacteria limit the range of *Prochlorococcus*. *Proceedings of the National Academy of Sciences of the United States of America*, *119*(2), 1–10. https://doi.org/10.1073/pnas.2110993118

Follows, M. J., Dutkiewicz, S., Grant, S., & Chisholm, S. W. (2007). Emergent biogeography of microbial communities in a model ocean. *Science*, *315*, 1843–1847. https://doi.org/10.1126/science.1138544

Gregg, W. W., & Casey, N. W. (2007). Modeling coccolithophores in the global oceans. *Deep Sea Research Part II: Topical Studies in Oceanography*, *54*(5), 447–477. https://doi.org/10.1016/j.dsr2.2006.12.007

Henson, S. A., Cael, B. B., Allen, S. R., & Dutkiewicz, S. (2021). Future phytoplankton diversity in a changing climate. *Nature Communications*, *12*(1), 1–8. https://doi.org/10.1038/s41467-021-25699-w

Holligan, P. M., Charalampopoulou, A., & Hutson, R. (2010). Seasonal distributions of the coccolithophore, *Emiliania huxleyi*, and of particulate inorganic carbon in surface waters of the Scotia Sea. *Journal of Marine Systems*, *82*(4), 195–205. https://doi.org/10.1016/j.jmarsys.2010.05.007

Holling, C. S. (1965). The functional response of predators to prey density and its role in mimicry and population regulation. *Memoirs of the Entomological Society of Canada*, *97*(Suppl. 45), 5–60. https://doi.org/10.4039/entm9745fv

Holzer, M., Primeau, W., Devries, T., & Matear, R. (2014). The Southern Ocean silicon trap: Data-constrained estimates of regenerated silicic acid, trapping efficiencies, and global transport paths. *Journal of Geophysical Research: Oceans*, *119*, 313–331. https://doi.org/10.1002/2013JC009356

Keeling, P. J. (2010). The endosymbiotic origin, diversification and fate of plastids. *Philosophical Transactions of the Royal Society B: Biological Sciences*, *365*(1541), 729–748. https://doi.org/10.1098/rstb.2009.0103

Kremer, C. T., Thomas, M. K., & Litchman, E. (2017). Temperature- and size-scaling of phytoplankton population growth rates: Reconciling the Eppley curve and the metabolic theory of ecology. *Limnology and Oceanography*, *62*(4), 1658–1670. https://doi.org/10.1002/lno.10523

Kwiatkowski, L., Torres, O., Bopp, L., Aumont, O., Chamberlain, M., Christian, R. J., Dunne, J. P., Gehlen, M., Ilyina, T., John, J. G., Lenton, A., Li, H., Lovenduski, N. S., Orr, J. C., Palmieri, J., Santana-Falcón, Y., Schwinger, J., Séférian, R., Stock, C. A., … Ziehn, T. (2020). Twenty-first century ocean warming, acidification, deoxygenation, and upper-ocean nutrient and primary production decline from CMIP6 model projections. *Biogeosciences*, *17*(13), 3439–3470. https://doi.org/10.5194/bg-17-3439-2020

Laufkotter, C., Vogt, M., Gruber, N., Aita-Noguchi, M., Aumont, O., Bopp, L., Buitenhuis, E., Doney, S. C., Dunne, J., Hashioka, T., Hauck, J., Hirata, T., John, J., Le Quéré, C., Lima, I. D., Nakano, H., Séférian, R., Totterdell, I., Vichi, M., & Volker, C. (2015). Drivers and uncertainties of future global marine primary production in marine ecosystem models. *Biogeosciences*, *12*(23), 6955–6984. https://doi.org/10.5194/bg-12-6955-2015

Le Quéré, C., Harrison, S. P., Prentice, I. C., Buitenhuis, E. T., Aumont, O., Bopp, L., Claustre, H., Cotrim Da Cunha, L., Geider, R., Giraud, X., Klaas, C., Kohfeld, K. E., Legendre, L., Manizza, M., Platt, T., Rivkin, R. B., Sathyendranath, S., Uitz, J., Watson, A. J., & Wolf-Gladrow, D. (2005). Ecosystem dynamics based on plankton functional types for global ocean biogeochemistry models. *Global Change Biology*, *2005*, 2016–2040. https://doi.org/10.1111/j.1365-2486.2005.1004.x

Leblanc, K., Arístegui Ruiz, J., Armand, L. K., Assmy, P., Beker, B., Bode, A., Breton, E., Cornet, V., Gibson, J., Gosselin, M. P., Kopczynska, E. E., Marshall, H. G., Peloquin, J. M., Piontkovski, S., Poulton, A. J., Quéguiner, B., Schiebel, R., Shipe, R., Stefels, J., … Yallop, M. (2012). Global distributions of diatoms abundance, biovolume and biomass—Gridded data product (NetCDF)—Contribution to the MAREDAT world ocean atlas of plankton functional types. *Pangaea*. https://doi.org/10.1594/PANGAEA.777384

Litchman, E., & Klausmeier, C. A. (2008). Trait-based community ecology of phytoplankton. *Annual Review of Ecology, Evolution, and Systematics*, *39*(1), 615–639. https://doi.org/10.1146/annurev.ecolsys.39.110707.173549

Marañón, E., Cermeño, P., López-Sandoval, D. C., Rodríguez-Ramos, T., Sobrino, C., Huete-Ortega, M., Blanco, J. M., & Rodríguez, J. (2013). Unimodal size scaling of phytoplankton growth and the size dependence of nutrient uptake and use. *Ecology Letters*, *16*(3), 371–379. https://doi.org/10.1111/ele.12052

Marañón, E., Lorenzo, M. P., Cermeño, P., & Mouriño-Carballido, B. (2018). Nutrient limitation suppresses the temperature dependence of phytoplankton metabolic rates. *ISME Journal*, *1–10*, 1836–1845. https://doi.org/10.1038/s41396-018-0105-1

Margalef, R. (1978). Life-forms of phytoplankton as survival alternatives in an unstable environment. *Oceanologica Acta*, *1*(4), 493–509.

Marinov, I., Doney, S. C., & Lima, I. D. (2010). Response of ocean phytoplankton community structure to climate change over the 21st century: Partitioning the effects of nutrients, temperature and light. *Biogeosciences*, *7*, 3941–3959. https://doi.org/10.5194/bg-7-3941-2010

Marshall, J., Adcroft, A., Hill, C., Perelman, L., & Heisey, C. (1997). A finite-volume, incompressible Navier stokes model for studies of the ocean on parallel computers. *Journal of Geophysical Research: Oceans*, *102*(C3), 5753–5766. https://doi.org/10.1029/96JC02775

Mitchell, C., Hu, C., Bowler, B., Drapeau, D., & Balch, W. M. (2017). Estimating particulate inorganic carbon concentrations of the global ocean from ocean color measurements using a reflectance difference approach. *Journal of Geophysical Research: Oceans*, *122*(11), 8707–8720. https://doi.org/10.1002/2017JC013146

Monier, E., Paltsev, S., Sokolov, A., Chen, Y. H. H., Gao, X., Ejaz, Q., Couzo, E., Schlosser, C. A., Dutkiewicz, S., Fant, C., Scott, J., Kicklighter, D., Morris, J., Jacoby, H., Prinn, R., & Haigh, M. (2018). Toward a consistent modeling framework to assess multi-sectoral climate impacts. *Nature Communications*, *9*(1), 1–8. https://doi.org/10.1038/s41467-018-02984-9

Monier, E., Scott, J. R., Sokolov, A. P., Forest, C. E., & Schlosser, C. A. (2013). An integrated assessment modeling framework for uncertainty studies in global and regional climate change: The MIT IGSM-CAM (version 1.0). *Geoscientific Model Development*, *6*(6), 2063–2085. https://doi.org/10.5194/gmd-6-2063-2013

Naselli-Flores, L., Zohary, T., & Padisák, J. (2021). Life in suspension and its impact on phytoplankton morphology: An homage to Colin S. Reynolds. *Hydrobiologia*, *848*(1), 7–30. https://doi.org/10.1007/s10750-020-04217-x

Negrete-García, G., Luo, J. Y., Long, M. C., Lindsay, K., Levy, M., & Barton, A. D. (2022). Plankton energy flows using a global size-structured and trait-based model. *Progress in Oceanography*, *209*, 102898. https://doi.org/10.1016/j.pocean.2022.102898

Nissen, C., Vogt, M., Münnich, M., Gruber, N., & Alexander Haumann, F. (2018). Factors controlling coccolithophore biogeography in the Southern Ocean. *Biogeosciences*, *15*(22), 6997–7024. https://doi.org/10.5194/bg-15-6997-2018

Padfield, D., Yvon-Durocher, G., Buckling, A., Jennings, S., & Yvon-Durocher, G. (2016). Rapid evolution of metabolic traits explains thermal adaptation in phytoplankton. *Ecology Letters*, *19*(2), 133–142. https://doi.org/10.1111/ele.12545

Raven, J. A. (1994). Why are there no picoplanktonic O2 evolvers with volumes less than 10^{-19} m^3? *Journal of Plankton Research*, *16*(5), 565–580. https://doi.org/10.1093/plankt/16.5.565

Reynolds, C. S., Huszar, V., Kruk, C., Naselli-Flores, L., & Melo, S. (2002). Towards a functional classification of the freshwater phytoplankton. *Journal of Plankton Research*, *24*(5), 417–428. https://doi.org/10.1093/plankt/24.5.417

Sherr, E. B., & Sherr, B. F. (1991). Planktonic microbes: Tiny cells at the base of the ocean's food webs. *Trends in Ecology & Evolution*, *6*(2), 50–54. https://doi.org/10.1016/0169-5347(91)90122-E

Shigemitsu, M., Okunishi, T., Nishioka, J., Sumata, H., Hashioka, T., Aita, M. N., Smith, S. L., Yoshie, N., Okada, N., & Yamanaka, Y. (2012). Development of a one-dimensional ecosystem model including the iron cycle applied to the Oyashio region, western subarctic Pacific. *Journal of Geophysical Research: Oceans*, *117*(6), 1–23. https://doi.org/10.1029/2011JC007689

Soppa, M. A., Hirata, T., Silva, B., Dinter, T., Peeken, I., Wiegmann, S., & Bracher, A. (2014). Global retrieval of diatom abundance based on phytoplankton pigments and satellite data. *Remote Sensing*, *6*(10), 10089–10106. https://doi.org/10.3390/rs61010089

Stock, C. A. (2019). Comparing apples to oranges: Perspectives on satellite-based primary production estimates drawn from a global biogeochemical model. *Journal of Marine Research*, *77*, 259–282.

Stock, C. A., Dunne, J. P., & John, J. G. (2014). Global-scale carbon and energy flows through the marine planktonic food web: An analysis with a coupled physical–biological model. *Progress in Oceanography*, *120*, 1–28. https://doi.org/10.1016/j.pocean.2013.07.001

Tang, E. P. Y. (1995). The allometry of algal growth rates. *Journal of Plankton Research*, *17*(2), 303–315. https://doi.org/10.1093/plankt/17.2.303

Thomas, M. K., Kremer, C. T., Klausmeier, C. A., & Litchman, E. (2012). A global pattern of thermal adaptation in marine phytoplankton. *Science*, *338*(6110), 1085–1088. https://doi.org/10.1126/science.1224836

Thomas, M. K., Kremer, C. T., & Litchman, E. (2016). Environment and evolutionary history determine the global biogeography of phytoplankton temperature traits. *Global Ecology and Biogeography*, *25*(1), 75–86. https://doi.org/10.1111/geb.12387

Toseland, A., Daines, S. J., Clark, J. R., Kirkham, A., Strauss, J., Uhlig, C., Lenton, T. M., Valentin, K., Pearson, G. A., Moulton, V., & Mock, T. (2013). The impact of temperature on marine phytoplankton resource allocation and metabolism. *Nature Climate Change*, *3*(11), 979–984. https://doi.org/10.1038/nclimate1989

Uitz, J., Claustre, H., Gentili, B., & Stramski, D. (2010). Phytoplankton class-specific primary production in the world's oceans: Seasonal and interannual variability from satellite observations. *Global Biogeochemical Cycles*, *24*(3), 1–19. https://doi.org/10.1029/2009GB003680

Uz, S. S., Brown, C. W., Heidinger, A. K., Smyth, T. J., & Murtugudde, R. (2013). Monitoring a sentinel species from satellites: Detecting *Emiliania huxleyi* in 25 years of AVHRR imagery. In J. Qu, A. Powell, & M. V. K. Sivakumar (Eds.), *Satellite-based applications on climate change* (pp. 277–288). Springer. https://doi.org/10.1007/978-94-007-5872-8_18

Ward, B. A., Dutkiewicz, S., Jahn, O., & Follows, M. J. (2012). A size-structured food-web model for the global ocean. *Limnology and Oceanography*, *57*(6), 1877–1891. https://doi.org/10.4319/lo.2012.57.6.1877

Ward, B. A., Marañón, E., Sauterey, B., Rault, J., & Claessen, D. (2017). The size dependence of phytoplankton growth rates: A trade-off between nutrient uptake and metabolism. *American Naturalist*, *189*(2), 170–177. https://doi.org/10.1086/689992

Willmer, P., Stone, G., & Johnston, I. (2004). *Environmental physiology of animals* (2nd ed.). Wiley-Blackwell.

Xi, H., Losa, S. N., Mangin, A., Soppa, M. A., Garnesson, P., Demaria, J., Liu, Y., Hembise Fanton d'Andon, O., & Bracher, A. (2020). Global retrieval of phytoplankton functional types based on empirical orthogonal functions using CMEMS GlobColour merged products and further extension to OLCI data. *Remote Sensing of Environment*, *240*, 111704. https://doi.org/10.1016/j.rse.2020.111704

SUPPORTING INFORMATION

Additional supporting information can be found online in the Supporting Information section at the end of this article.

How to cite this article: Anderson, S. I., Fronda, C., Barton, A. D., Clayton, S., Rynearson, T. A., & Dutkiewicz, S. (2023). Phytoplankton thermal trait parameterization alters community structure and biogeochemical processes in a modeled ocean. *Global Change Biology*, *30*, e17093. https://doi.org/10.1111/gcb.17093